Identification of effective CCR2 inhibitors for cancer therapy using humanized mice

杉山, 成明

Rapid Communication / Biochemistry

Identification of effective CCR2 inhibitors for cancer therapy using humanized mice

Shigeaki Sugiyama[1], Kanae Yumimoto[1], Shun Fujinuma[1], Keiichi I. Nakayama[1,2,†]

[1]Department of Molecular and Cellular Biology, Medical Institute of Bioregulation, Kyushu University, 3-1-1 Maidashi, Higashi-ku, Fukuoka, Fukuoka 812-8582, Japan; [2]Anticancer Strategies Laboratory, TMDU Advanced Research Institute, Tokyo Medical and Dental University, 1-5-45 Yushima, Bunkyo-ku, Tokyo 113-8510, Japan.

[†]Keiichi I. Nakayama: Department of Molecular and Cellular Biology, Medical Institute of Bioregulation, Kyushu University, 3-1-1 Maidashi, Higashi-ku, Fukuoka, Fukuoka 812-8582, Japan. Tel.: +81-92-642-6815, Fax: +81-92-642-6819, e-mail: nakayak1@bioreg.kyushu-u.ac.jp

Running head: Effective CCR2 inhibitors for cancer therapy

Abbreviations: Bregs, regulatory B cells; CCL2, C‐C motif chemokine 2; CCR2, C-C chemokine receptor type 2; IC_{50}, 50% inhibitory concentration; M-MDSCs, monocytic myeloid-derived suppressor cells; PMN-MDSCs, polymorphonuclear myeloid-derived suppressor cells; TAMs, tumor-associated macrophages; Tregs, regulatory T cells.

Abstract

C-C chemokine receptor type 2 (CCR2) is the receptor for C-C motif chemokine 2 (CCL2) and is associated with various inflammatory diseases and cancer metastasis. Although many inhibitors for CCR2 have been developed, it remains unresolved which inhibitors are the most effective in the clinical setting. In the present study, we compared 10 existing human CCR2 antagonists in a calcium influx assay using human monocytic leukemia cells. Among them, MK0812 was found to be the most potent inhibitor of human CCR2. Furthermore, we generated a human *CCR2B* knock-in mouse model to test the efficacy of MK0812 against a lung metastasis model of breast cancer. Oral administration of MK0812 to humanized mice did indeed reduce the number of monocytic myeloid-derived suppressor cells and the rate of lung metastasis. These results suggest that MK0812 is the most promising candidate among the commercially available CCR2 inhibitors. We propose that combining these two screening methods may provide an excellent experimental method for identifying effective drugs that inhibit human CCR2.

Keywords: cancer metastasis; C-C chemokine receptor type 2 (CCR2); knockout mice; knock-in mice; monocytic myeloid-derived suppressor cells (M-MDSCs)

The cancer niche is the microenvironment that supports the proliferation, invasion, and metastasis of cancer cells. It includes immune cells such as tumor-associated macrophages (TAMs), polymorphonuclear myeloid-derived suppressor cells (PMN-MDSCs), monocytic myeloid-derived suppressor cells (M-MDSCs), regulatory T cells (Tregs), and regulatory B cells (Bregs). Typically, immune cells eliminate cancer cells, but as cancer progresses, the cancer cells educate these immune cells through molecules such as cytokines and chemokines. This in turn transforms the cells surrounding the cancer into cells that promote cancer progression, creating a microenvironment favorable for cancer cell growth and metastasis (*1*).

M-MDSCs promote tumor development and metastasis by inhibiting T cells through the action of various molecules (*2, 3*), such as IL-10, TGF- β, and CD40, which induce the differentiation of CD4 T cells into Tregs (*4, 5*). M-MDSCs also produce arginase 1, which decreases the levels of L-arginine, an amino acid essential for T-cell response (*6*). Additionally, they metabolize tryptophan into kynurenine through indoleamine 2, 3-dioxygenase, which inhibits T cell proliferation (*7*). Programmed cell death-ligand 1 (PD-L1) and cytotoxic T lymphocyte-associated antigen 4 (CTLA-4), both of which can inhibit T cells through cell-cell interaction, are both expressed on MDSCs (*3*).

The C-C chemokine receptor type 2 (CCR2) and its ligand, C-C motif chemokine 2 (CCL2, also known as monocyte chemotaxis protein 1), have attracted the interest of many researchers because of their potential role in cancer progression. (*8*). M-MDSCs are induced by both tumor-derived and stromal-derived CCL2 to transform into TAMs in the tumor microenvironment, resulting in the formation of a cancer niche (*9, 10*). Subcutaneous transplantation of LLC1 (Lewis lung carcinoma) cells into CCR2-deficient mice reduced the number of TAM in the lungs and suppressed lung metastasis compared with wild-type mice (*11, 12*). Some studies have shown that CCR2 inhibitors can suppress tumor growth by preventing the accumulation of M-MDSCs at the tumor site. For instance, propagermanium, a CCR2 inhibitor, was found to inhibit the spread of melanoma cell lines to the lungs by reducing the number of M-MDSCs in the lungs (*10*). Likewise, PF04136309, another CCR2 inhibitor, showed antitumor effects by inhibiting the accumulation of M-MDSCs and TAMs in a mouse model of pancreatic ductal adenocarcinoma (*13*).

CCR2 has been considered a promising therapeutic target for cancer, as well as diabetes and multiple sclerosis (*8, 14, 15*). Several CCR2 inhibitors have been developed and tested in clinical trials (*16*). A Phase Ib study was conducted to evaluate the efficacy of the CCR2 inhibitor PF-04136309 in combination with

FOLFIRINOX in patients with borderline resectable and locally advanced pancreatic cancer (NCT01413022) (*17*). The study showed that toxicity was manageable and tolerable, and partial responses (PR) were achieved in 48% of patients. However, given that human and mouse CCR2 are structurally different and that many of the antagonists developed have been ineffective against mouse CCR2, it is technically difficult to determine the clinical efficacy of each CCR2 inhibitor using mouse models.

In the present study, we first conducted a calcium influx assay using human monocytic leukemia cells. MK0812 was identified as the most potent antagonist of human CCR2 in the calcium influx assay. Its IC_{50} (50% inhibitory concentration) value was approximately four times lower than that of PF04136309, which showed therapeutic efficacy in clinical trials for pancreatic cancer (*17*). To further evaluate the pharmacokinetics and efficacy of MK0812, we generated human *CCR2B* knock-in mice. Oral administration of MK0812 inhibited the accumulation of M-MDSCs in the lungs, and showed a therapeutic effect in a breast cancer lung metastasis model. These results indicate that MK0812 has excellent potential as a therapeutic candidate for inhibiting human CCR2. Moreover, our human *CCR2B* knock-in mice constitute a valuable preclinical model to evaluate the effectiveness of CCR2 antagonists in treating various conditions.

Materials and methods

Nucleotides

A list of the nucleotides used in the study is provided in Table 1.

Animals

All animal experiments were approved by the animal ethics committee of Kyushu University (approval code A22-242-0) and were conducted in compliance with university guidelines and regulations for animal experimentation. Mice were housed in the specific pathogen–free animal facility at Kyushu University following institutional guidelines and under the following conditions: ambient temperature of 22°C, humidity of 50 to 60%, 12-hour light/12-hour dark cycle, and free access to water and rodent chow (CA-1, CLEA Japan) as described previously (*18*). All experiments were performed with female mice aged between eight to twelve weeks on the C57BL/6J background. C57BL/6J mice were obtained from The Jackson Laboratory.

Generation of human CCR2B knock-in mice

The targeting vector for *CCR2* was constructed by replacement of a 1.1-kbp fragment of genomic DNA containing exons III of the *CCR2* gene with a human *CCR2B* cassette, as shown in Figure 3A. This vector was electroporated into ES (embryonic stem) cells with the pX330-U6-Chimeric_BB-CBh-hSpCas9 vector encoding Cas9 protein and guide RNA sequences (Table 1). Human *CCR2B* knock-in ES cells were obtained by PCR analysis of cloned ES cells. To confirm that non-specific incorporation of the human *CCR2B* allele into the genome has not occurred, DNA prepared from PCR-positive clones was digested with BamHI, transferred to a nylon membrane, and then subjected to Southern blot analysis with the probes. Human *CCR2B* knock-in ES cells were microinjected into C57BL/6J blastocysts, and resulting male chimeras were mated with C57BL/6J mice. Germ-line transmission of the human *CCR2B* allele was confirmed by PCR analysis. Heterozygous offspring were intercrossed to produce homozygous knock-in mice.

Generation of mouse CCR2 knockout mice

Ribonucleoprotein (RNP) was prepared by mixing the CRISPR RNA (crRNA) (Table 1) and transactivating crRNA (tracrRNA) with recombinant Cas9 protein (Integrated DNA Technologies). Mouse zygotes of the C57BL/6J strain were subjected to electroporation with RNP. DNA from mosaic offspring tails was used to identify *CCR2* mutant mice by T7E1 assay and Sanger sequencing. *CCR2* mutant offspring were mated with C57BL/6J mice. PCR analysis confirmed the germ-line transmission of the *CCR2* mutant allele (Table 1). Heterozygous offspring were intercrossed to produce homozygous knockout mice.

T7E1 assay

PCR products using DNA from mouse tail were denatured in NEBuffer 2 (New England Biolabs), reannealed, treated with T7 Endonuclease I (New England Biolabs) at 37°C for 30 min, and run on 0.75% agarose gel. Primer sequences used for PCR are shown in Table 1.

Cell culture

E0771 (CH3 BioSystems) cells were maintained at 37°C in RPMI 1640 medium (Sigma-Aldrich) supplemented with 10% fetal bovine serum (Invitrogen), 1 mM sodium pyruvate, 100 U/ml penicillin, 100

126 μg/ml streptomycin, 2 mM L-glutamine, and ten ml/l nonessential amino acids (Gibco), 10 mM HEPES
127 (Sigma-Aldrich).
128
129 ***Lung metastasis model and therapeutic experiment***
130 Tumor cells (5×10^5 E0771 cells) were injected into the tail vein of mice. Mice were perfused with PBS
131 (heparin 10 U/ml), and lungs were removed. MK0812 (TargetMol) was dissolved in dimethyl sulfoxide
132 (DMSO) and corn oil and administered orally (15 mg/kg twice daily) for eight days.
133
134 ***Flow cytometry***
135 Flow cytometry analysis was performed as described previously (*18*). Single-cell suspensions were obtained
136 from the lung by digestion with collagenase (1 mg/ml) (Wako) at 37 °C for 60 min, followed by passing
137 through a 70-μm cell strainer and lysis of red blood cells (0.14 M NH_4Cl and 0.01 M Tris-HCl at pH 7.5) for 5
138 min at room temperature. Bone marrow mononuclear cells flushed from the tibia and femur of mice were
139 suspended in Hanks' balanced salt solution (HBSS) and lysed (0.14 M NH_4Cl and 0.01 M Tris-HCl at pH 7.5)
140 for 10 min at room temperature. The isolated cells were Fc-blocked for 15 min with anti-CD16/32 (2.4G2, BD
141 Biosciences) and stained with antibodies to CD45.2 (104, BioLegend), to CD11b (M1/70, BioLegend), to
142 Ly6G (1A8, BioLegend) and Ly6C (AL-21, BD Biosciences) for 30 min. The stained cells were treated with
143 7-AAD (BD Biosciences) to exclude dead cells and analyzed with a FACSVerse, FACSAria, or
144 FACSymphony A1 flow cytometer (Becton Dickinson).
145
146 ***Calcium influx assay***
147 THP-1 cell line (in HBSS with 0.05% BSA) was incubated with Fure 2-AM (final concentration 5.0 μM) for
148 30 min at 37°C in the dark, washed twice with HBSS with 0.05% BSA and added each CCR2 inhibitor
149 (MK0812 (Cayman), PF04634817 (Sigma-Aldrich), PF04136309 (PharmaBlock), INCB3344 (Chemscene),
150 Cenicriviroc (Axon), JNJ2714149 (R&D systems), CCR2-RA-[R] (MedChemExpress), CAS-445479-97-0
151 (Santa Cruz Biotechnology), RS504393 (Sigma-Aldrich) and RS102895 (Sigma-Aldrich)). After 30 min of
152 incubation, recombinant Human CCL2 (BioLegend) prepared at 50 nM in HBSS with 0.2% BSA was applied,
153 and fluorescence was detected by FDSS 7000EX (Hamamatsu Photonics). The ratio of Fluorescence

(excitation at 340 nm, emission at 540 nm) to Fluorescence (excitation at 380 nm, emission at 540 nm) at each time point was subtracted from that before CCL2 application, and the IC_{50} was calculated based on the maximum value.

Statistical analysis

Quantitative data were subjected to statistical analysis as indicated and are presented as means ± SEM. A P value less than 0.05 was considered statistically significant.

Results

Lung metastasis of breast cancer is suppressed in CCR2 knockout mice

To confirm CCR2 as a therapeutic target for breast cancer lung metastasis in mice, we first generated *CCR2* knockout (*CCR2* KO) mice. CRISPR RNA (crRNA) consisting of guide RNA and RNA complementary to transactivating crRNA (tracrRNA) was electroporated into mouse zygotes with tracrRNA and Cas9 protein. The guide RNA was designed to target sequences near the 5' end of the *CCR2* open reading frame (ORF) (Fig. 1A). The *CCR2* ORF region was amplified by PCR using DNA from the tails of mice obtained by CRISPR/Cas9 electroporation (Fig. 1A), and the T7E1 assay was performed (Fig. 1B). Finally, one mosaic mouse was found with a 5 bp deletion in the ORF region of CCR2, indicating that only the short truncated protein is translated by frameshift (Fig. 1C). This *CCR2* mutant mosaic mouse was crossed with C57BL/6J mice, and heterozygous offspring were intercrossed to produce homozygous mice. We confirmed the deficiency of CCR2 by flow cytometry analysis of bone marrow cells from these homozygous mice (Fig. 1D). We recovered lung cells from these *CCR2* knockout mice and performed flow cytometry analysis confirming that the number of M-MDSCs ($CD45^+CD11b^+Ly6G^-Ly6C^+$ cells) in the lung was reduced compared with that of wild-type mice (Fig. 1E).

We previously showed that the CCR2 antagonist propagermanium suppressed spontaneous metastasis of the breast cancer cell line E0771 by inhibiting the accumulation of M-MDSCs (*10*). To test whether lung metastasis of breast cancer cells is also suppressed in *CCR2* knockout mice, we injected E0771 cells stably overexpressing the fluorescent protein tdTomato through the tail vein of the mice, and lung metastasis was evaluated (Fig. 1F). We confirmed that lung metastasis was indeed suppressed in *CCR2*

knockout mice compared with wild-type mice (Fig. 1G). These results suggest that the tail vein injection of the E0771 breast cancer cell line can be used as a useful evaluation system for CCR2 inhibitors targeting lung metastasis.

MK0812 is the most potent human CCR2 inhibitor

CCR2 is a therapeutic target molecule for various diseases including cancer, and many inhibitors have been developed to date (*8, 14-16*). However, each has been tested in independent experimental systems and not analyzed in a unified manner. We therefore compared the efficacy of 10 commercially available human CCR2 inhibitors (MK0812, PF04634817, PF04136309, INCB3344, Cenicriviroc, JNJ2714149, CCR2-RA-[R], CAS-445479-97-0, RS504393, and RS102895). CCR2 is a G protein-coupled receptor (GPCR), and binding of its ligand, CCL2, activates phospholipase C, resulting in calcium influx from the endoplasmic reticulum into the cytoplasm (*19*). We quantified the inhibitory activity of human CCR2 inhibitors using THP-1, a human monocytic leukemia cell line known to express CCR2 (*20*). Fura2-AM, a Ca^{2+} selective fluorescent indicator, was incorporated into THP-1 cells, treated with each human CCR2 inhibitor and recombinant human CCL2, and fluorescence was monitored by FDSS 7000EX (Fig. 2A and 2B). Among the CCR2 inhibitors, MK0812 showed the lowest IC_{50} (1.73 nM), about 4-fold lower than PF04136309 (IC_{50}=6.99 nM) (Fig. 2C), which showed a response in borderline resectable and locally advanced pancreatic cancer (*17*). RS102895 did not show 50% inhibition within the concentrations used in this study, so its IC_{50} could not be calculated and is not shown in Figure 2C. Although no clinical trials of MK0812 on cancer have performed to date, we propose that this compound may be a promising anticancer agent.

Generation of human CCR2B knock-in mice

Two splicing variants of human CCR2 (CCR2A and CCR2B) are present, and that most CCR2 expressed on the plasma membrane of hematopoietic cells is CCR2B (*21*). Also, human peripheral blood monocytes and mouse peritoneal macrophages expressing human CCR2B exhibit chemotaxis to mouse CCL2 (*22*). In addition, treatment with the CCR2 antagonist CCX140-B reduced the number of inflammatory macrophages in adipose tissue and decreased fasting blood glucose and insulin levels (*23*).

To verify the anti-tumor effect of MK0812 *in vivo*, we generated mice in which the endogenous *CCR2* ORF was replaced with human *CCR2B* ORF (hereafter referred to as human *CCR2B* knock-in mice). Vectors encoding the human *CCR2B* ORF and the homologous arm for mouse *CCR2* were electroporated into embryonic stem (ES) cells with vectors encoding Cas9 and guide RNA sequences (Fig. 3A). Human *CCR2B* knock-in ES cells (Clone #29) were obtained by PCR genotyping of cloned ES cells (Fig. 3B). Southern blot analysis revealed no nonspecific incorporation of human *CCR2B* into the mouse genome (Fig. 3C). Chimeric mice (F0 generation) were obtained by microinjection of the human *CCR2B* knock-in ES cells into blastocysts (Fig. 3D). Next, the F1 generation was obtained by mating the chimeric mice with wild-type C57BL/6 mice, and the propagation of the ES cells to the germ line was confirmed by their coat color (Fig. 3E). The F1 generation was then genotyped to verify that human *CCR2B* was indeed knocked in the mouse *CCR2* locus (Fig. 3F). Heterozygous offspring were intercrossed to produce homozygous human *CCR2B* knock-in mice. We analyzed bone marrow cells from these homozygous mice by flow cytometry and confirmed the expression of human CCR2 (Fig. 3G).

MK0812 suppresses cancer metastasis in humanized mice

We next tried to examine whether MK0812 inhibits cancer metastasis *in vivo*. We injected the tdTomato-labeled E0771 cancer cell line into the tail vein of human *CCR2B* knock-in mice, and MK0812 was orally administered (15 mg/kg, twice daily) for eight days starting two days later (Fig. 4A). We performed flow cytometry analysis of lung cells and found that the number of M-MDSCs were significantly reduced in mice treated with MK0812 compared with control mice. Correspondingly, MK0812 treatment also suppressed lung metastasis of E0771 cells in human *CCR2B* knock-in mice (Fig. 4B and 4C). No apparent side effects or weight loss were observed in mice treated with MK0812. These results suggest that MK0812 has therapeutic potential in clinical human cancer metastasis.

Discussion

CCR2 is a chemokine receptor that plays a key role in monocyte infiltration and tumor immunity in response to CCL2. The CCR2-CCL2 axis has been considered a promising target for cancer treatment, and many inhibitors for CCR2 have been developed, with some undergoing clinical trials (*16*). However, the

development of potent inhibitors for CCR2 has been hampered by the lack of animal models to assess the efficacy of inhibitors in the clinical setting. In the present study, we examined the effectiveness of 10 human CCR2 inhibitors using two screening methods, a calcium influx assay using human monocytic leukemia cells and cancer metastasis assay using human *CCR2B* knock-in mice. Our results indicate that MK0812 is the most potent inhibitor of human CCR2, outperforming drugs such as PF04136309 and Cenicriviroc, which are in the clinical trials (*17, 24*). Oral administration of MK0812 to human *CCR2B* knock-in mice did not result in weight loss or other serious side effects, despite remarkable efficacy of this drug in suppressing lung metastases. We have also listed each inhibitor by IC_{50}, providing new insights into future CCR2 antagonist development based on structural and other information.

Furthermore, CCR2 serves as a potential therapeutic target for an array of inflammation-related diseases, including diabetes, lupus nephritis, non-alcoholic steatohepatitis, chronic obstructive pulmonary disease, and primary sclerosing cholangitis (PSC) (*15, 25-28*). In phase II clinical trials, Cenicriviroc demonstrated only moderate improvement in PSC (*24*). Given that Cenicriviroc is a 16-fold weaker inhibitor than MK0812 in our calcium influx assay, more potent CCR2 antagonists may effectively treat various inflammation-related diseases.

There are some limitations to this study that need to be considered. Firstly, not all CCR2 inhibitors were examined in the cancer metastasis model using human *CCR2B* knock-in mice, and the IC_{50} of CCR2 inhibitors was only determined through the calcium influx assay. Given that propagermanium was shown to block the migratory properties of CCL2 without inhibiting calcium influx into the cell (*29*), however, our calcium influx assays may not be able to assess anti-CCR2 effects for some drugs. Second, the pharmacokinetics of drugs in human *CCR2B* knock-in mice may not reflect their pharmacokinetics in humans.

To summarize our findings, MK0812 showed the most potential as a CCR2 antagonist out of 10 candidates. Without any side effects, it effectively suppressed breast cancer lung metastasis in human *CCR2B* knock-in mice. This finding could aid in the development of future drugs that inhibit the CCL2-CCR2 axis for a number of diseases.

Funding

This work was supported in part by Research Support Project for Life Science and Drug Discovery (Basis for Supporting Innovative Drug Discovery and Life Science Research (BINDS)) from Japan Agency for Medical Research and Development (AMED) under Grant Number JP21am0101091 (support number 1751). This work was also supported by KAKENHI grants from the Japan Society for the Promotion of Science (JSPS) to K.I.N. (JP23H00378) and to K.Y. (JP20K07592 and JP19J40055) and the FOREST Program of the Japan Science and Technology Agency to K.Y (JPMJFR216G).

Conflict of interest

The authors declare that they have no competing interests.

Acknowledgements

We thank for technical assistance; T. Yamashita, Y. Okabe, A. Matsukuma, B. Donahue, and A. Ohta for their help with the preparation of the manuscript.

REFERENCES

1. Barcellos-Hoff, M.H., Lyden, D., and Wang, T.C. (2013) The evolution of the cancer niche during multistage carcinogenesis. *Nat. Rev. Cancer*. **13**, 511-518
2. Li, Y., He, H., Jihu, R., Zhou, J., Zeng, R., and Yan, H. (2021) Novel characterization of myeloid-derived suppressor cells in tumor microenvironment. *Front. Cell Dev. Biol*. **9**, 698532
3. Yang, Y., Li, C., Liu, T., Dai, X., and Bazhin, A.V. (2020) Myeloid-derived suppressor cells in tumors: from mechanisms to antigen specificity and microenvironmental regulation. *Front. Immunol.* **11**, 1371
4. Huang, B., Pan, P.Y., Li, Q., Sato, A.I., Levy, D.E., Bromberg, J., Divino, C.M., and Chen, S.H. (2006) Gr-1^{+}CD115^{+} immature myeloid suppressor cells mediate the development of tumor-induced T regulatory cells and T-cell anergy in tumor-bearing host. *Cancer Res.* **66**, 1123-1131
5. Pan, P.Y., Ma, G., Weber, K.J., Ozao-Choy, J., Wang, G., Yin, B., Divino, C.M., and Chen, S.H. (2010) Immune stimulatory receptor CD40 is required for T-cell suppression and T regulatory cell activation mediated by myeloid-derived suppressor cells in cancer. *Cancer Res.* **70**, 99-108
6. Rodríguez, P.C., and Ochoa, A.C. (2008) Arginine regulation by myeloid derived suppressor cells and tolerance in cancer: mechanisms and therapeutic perspectives. *Immunol. Rev.* **222**, 180-191
7. Peyraud, F., Guegan, J.P., Bodet, D., Cousin, S., Bessede, A., and Italiano, A. (2022) Targeting tryptophan catabolism in cancer immunotherapy era: challenges and perspectives. *Front. Immunol.* **13**, 807271
8. Lim, S.Y., Yuzhalin, A.E., Gordon-Weeks, A.N., and Muschel, R.J. (2016) Targeting the CCL2-CCR2 signaling axis in cancer metastasis. *Oncotarget*. **7**, 28697-28710
9. Chang, A.L., Miska, J., Wainwright, D.A., Dey, M., Rivetta, C.V., Yu, D., Kanojia, D., Pituch, K.C., Qiao, J., Pytel, P., Han, Y., Wu, M., Zhang, L., Horbinski, C.M., Ahmed, A.U., and Lesniak, M.S. (2016) CCL2 produced by the glioma microenvironment is essential for the recruitment of regulatory T cells and myeloid-derived suppressor cells. *Cancer Res.* **76**, 5671-5682
10. Yumimoto, K., Akiyoshi, S., Ueo, H., Sagara, Y., Onoyama, I., Ueo, H., Ohno, S., Mori, M., Mimori, K., and Nakayama, K.I. (2015) F-box protein FBXW7 inhibits cancer metastasis in a non-cell-autonomous manner. *J. Clin. Invest.* **125**, 621-635
11. Kumar, V., and Gabrilovich, D.I. (2014) Hypoxia-inducible factors in regulation of immune responses

in tumour microenvironment. *Immunology*. **143**, 512-519

12. Schmall, A., Al-Tamari, H.M., Herold, S., Kampschulte, M., Weigert, A., Wietelmann, A., Vipotnik, N., Grimminger, F., Seeger, W., Pullamsetti, S.S., and Savai, R. (2015) Macrophage and cancer cell cross-talk via CCR2 and CX3CR1 is a fundamental mechanism driving lung cancer. *Am. J. Respir. Crit. Care Med*. **191**, 437-447

13. Mitchem, J.B., Brennan, D.J., Knolhoff, B.L., Belt, B.A., Zhu, Y., Sanford, D.E., Belaygorod, L., Carpenter, D., Collins, L., Piwnica-Worms, D., Hewitt, S., Udupi, G.M., Gallagher, W.M., Wegner, C., West, B.L., Wang-Gillam, A., Goedegebuure, P., Linehan, D.C., and DeNardo, D.G. (2013) Targeting tumor-infiltrating macrophages decreases tumor-initiating cells, relieves immunosuppression, and improves chemotherapeutic responses. *Cancer Res.* **73**, 1128-1141

14. Cui, L.Y., Chu, S.F., and Chen, N.H. (2020) The role of chemokines and chemokine receptors in multiple sclerosis. *Int. Immunopharmacol.* **83**, 106314

15. Seok, S.J., Lee, E.S., Kim, G.T., Hyun, M., Lee, J.H., Chen, S., Choi, R., Kim, H.M., Lee, E.Y., and Chung, C.H. (2013) Blockade of CCL2/CCR2 signalling ameliorates diabetic nephropathy in db/db mice. *Nephrol. Dial. Transplant*. **28**, 1700-1710

16. Yumimoto, K., Sugiyama, S., Mimori, K., and Nakayama, K.I. (2019) Potentials of C-C motif chemokine 2-C-C chemokine receptor type 2 blockers including propagermanium as anticancer agents. *Cancer Sci.* **110**, 2090-2099

17. Nywening, T.M., Wang-Gillam, A., Sanford, D.E., Belt, B.A., Panni, R.Z., Cusworth, B.M., Toriola, A.T., Nieman, R.K., Worley, L.A., Yano, M., Fowler, K.J., Lockhart, A.C., Suresh, R., Tan, B.R., Lim, K.H., Fields, R.C., Strasberg, S.M., Hawkins, W.G., DeNardo, D.G., Goedegebuure, S.P., and Linehan, D.C. (2016) Targeting tumour-associated macrophages with CCR2 inhibition in combination with FOLFIRINOX in patients with borderline resectable and locally advanced pancreatic cancer: a single-centre, open-label, dose-finding, non-randomised, phase 1b trial. *Lancet Oncol.* **17**, 651-662

18. Yumimoto, K., Sugiyama, S., Motomura, S., Takahashi, D., and Nakayama, K.I. (2023) Molecular evolution of Keap1 was essential for adaptation of vertebrates to terrestrial life. *Sci. Adv*. **9**, eadg2379

19. Fei, L., Ren, X., Yu, H., and Zhan, Y. (2021) Targeting the CCL2/CCR2 axis in cancer immunotherapy: one stone, three birds? *Front. Immunol.* **12**, 771210

20. Phillips, R.J., Lutz, M., and Premack, B. (2005) Differential signaling mechanisms regulate expression of CC chemokine receptor-2 during monocyte maturation. *J. Inflamm. (Lond.)*. **2**, 14

21. Charo, I.F., Myers, S.J., Herman, A., Franci, C., Connolly, A.J., and Coughlin, S.R. (1994) Molecular cloning and functional expression of two monocyte chemoattractant protein 1 receptors reveals alternative splicing of the carboxyl-terminal tails. *Proc. Natl. Acad. Sci. U. S. A.* **91**, 2752-2756

22. Prosser, H.M., Cooper, D.G., Forbes, I.T., Geppert, M., Gribble, A.D., Grau, E.V., Groot, P.H., Harper, A.J., Moores, K.E., Pickering, S.J., and Piercy, V. (2002) Targeted replacement of rodent CCR2 with the human orthologue CCR2B: A mouse model for in vivo analysis of human target-selective small molecule MCP-1 receptor antagonists. *Drug Dev. Res.* **55**, 197-209

23. Sullivan, T., Miao, Z., Dairaghi, D.J., Krasinski, A., Wang, Y., Zhao, B.N., Baumgart, T., Ertl, L.S., Pennell, A., Seitz, L., Powers, J., Zhao, R., Ungashe, S., Wei, Z., Boring, L., Tsou, C.L., Charo, I., Berahovich, R.D., Schall, T.J., and Jaen, J.C. (2013) CCR2 antagonist CCX140-B provides renal and glycemic benefits in diabetic transgenic human CCR2 knockin mice. *Am. J. Physiol. Renal Physiol.* **305**, F1288-1297

24. Eksteen, B., Bowlus, C.L., Montano-Loza, A.J., Lefebvre, E., Fischer, L., Vig, P., Martins, E.B., Ahmad, J., Yimam, K.K., Pockros, P.J., Feld, J.J., Minuk, G., and Levy, C. (2021) Efficacy and safety of cenicriviroc in patients with primary sclerosing cholangitis: PERSEUS study. *Hepatol Commun*. **5**, 478-490

25. Guicciardi, M.E., Trussoni, C.E., Krishnan, A., Bronk, S.F., Lorenzo Pisarello, M.J., O'Hara, S.P., Splinter, P.L., Gao, Y., Vig, P., Revzin, A., LaRusso, N.F., and Gores, G.J. (2018) Macrophages contribute to the pathogenesis of sclerosing cholangitis in mice. *J. Hepatol.* **69**, 676-686

26. Henrot, P., Prevel, R., Berger, P., and Dupin, I. (2019) Chemokines in COPD: from implication to therapeutic use. *Int. J. Mol. Sci.* **20**, 2785

27. Miura, K., Yang, L., van Rooijen, N., Ohnishi, H., and Seki, E. (2012) Hepatic recruitment of macrophages promotes nonalcoholic steatohepatitis through CCR2. *Am. J. Physiol. Gastrointest. Liver Physiol.* **302**, G1310-1321

28. Pérez de Lema, G., Maier, H., Franz, T.J., Escribese, M., Chilla, S., Segerer, S., Camarasa, N., Schmid, H., Banas, B., Kalaydjiev, S., Busch, D.H., Pfeffer, K., Mampaso, F., Schlöndorff, D., and Luckow, B.

(2005) Chemokine receptor Ccr2 deficiency reduces renal disease and prolongs survival in MRL/lpr lupus-prone mice. *J. Am. Soc. Nephrol.* **16**, 3592-3601

29. Yokochi, S., Hashimoto, H., Ishiwata, Y., Shimokawa, H., Haino, M., Terashima, Y., and Matsushima, K. (2001) An anti-inflammatory drug, propagermanium, may target GPI-anchored proteins associated with an MCP-1 receptor, CCR2. *J Interferon Cytokine Res*. **21**, 389-398

Figure legends

Fig. 1. CCR2 inhibition suppresses lung metastasis of breast cancer cell line. (A) Strategy for generating mouse *CCR2* knockout mice by CRISPR/Cas9 electroporation. The target sequence of the guide RNA was designed on the 5' end side of the mouse *CCR2* ORF (open reading frame). Ribonucleoprotein was prepared by mixing the CRISPR RNA (Table 1) and transactivating crRNA with recombinant Cas9 protein. Mouse zygotes of the C57BL/6J strain were subjected to electroporation with RNP. (B) T7E1 assay of mosaic mice obtained by CRISPR/Cas9 electroporation in Figure 1A. The *CCR2* ORF regions of mosaic and wild-type mice were amplified by PCR using DNA obtained from the tails, and the PCR products were denatured, reannealed, and treated with T7E1 endonuclease I. *CCR2* mutations were found in mouse #6 (shown in red). (C) Sanger sequencing the mouse *CCR2* ORF region in mouse #6. (D) Flow cytometry analysis of bone marrow cells recovered from wild-type and *CCR2* knockout (KO) mice using anti-mouse CCR2 (Anti-mCCR2) antibody. (E) Flow cytometry analysis of lung M-MDSCs in wild-type and *CCR2* KO mice. ***$p < 0.001$ (unpaired two-sided Student's t-test). ($N = 4$). (F) Schematic representation of breast cancer cells' lung metastasis evaluation assay. Wild-type or *CCR2* KO mice were injected with tdTomato-labeled E0771 cancer cell line into the tail vein, and 14 days later, lungs were removed and evaluated for tdTomato-positive lung metastases. (G) Lung metastases were evaluated 14 days after tail vein injection of tdTomato-labeled E0771 cancer cell line. Lungs were photographed under blue light irradiation (left). The percentage of tdTomato-positive area in the lung was quantitated with ImageJ software. (right). ***$p < 0.001$ (unpaired two-sided Student's t-test). Scale bars: 5 mm. ($N = 15$ for Wild-type; $N = 9$ for *CCR2* KO).

Fig. 2. MK0812 is the most potent human CCR2 inhibitor. (A) Schematic diagram of human CCR2 inhibitor screening. (B) Fura 2-AM-incorporated THP-1 cell lines were stimulated with each human CCR2 inhibitor and recombinant human CCL2, and fluorescence was detected. The vertical axis is the ratio of Fluorescence (excitation at 340 nm, emission at 540 nm) to Fluorescence (excitation at 380 nm, emission at 540 nm) at each time point. (C) IC_{50} summary calculated based on the results in (B) ($N = 3$).

Fig. 3. Generation of human *CCR2B* knock-in mice. (A) Strategy for generating human *CCR2B* knock-in ES cells by homologous recombination. The human *CCR2B* knock-in construct consists of human *CCR2B*

ORF (open reading frame) and HA (homologous arm). (B) Genotyping of cloned ES cells by PCR. Knock-in of the human *CCR2B* allele was confirmed in clone #29 (shown in red). (C) Southern blot analysis of DNA from human *CCR2B* knock-in ES cells (clone #29). (D) F0 generation chimeric mice were obtained by microinjection of clone #29 into blastocysts. (E) F1 generation mice were obtained by crossing F0 generation chimeric mice with C57BL/6J mice. (F) Genotyping of F1 generation mice by PCR. N.C., negative control, P.C., positive control. DNA extracted from wild-type C57BL/6 mice was used as N.C. DNA extracted from chimeric mice in Figure 4D as P.C. (G) Flow cytometry analysis of bone marrow cells recovered from wild-type and human *CCR2B* knock-in (indicated as h*CCR2B* KI) mice using anti-mouse CCR2 (shown as Anti-mCCR2) or anti-human CCR2 (shown as Anti-hCCR2) antibodies.

Fig. 4. MK0812 inhibits the accumulation of M-MDSCs and suppresses cancer metastasis in human *CCR2B* knock-in mice. (A) Schematic lung metastasis evaluation assay representation using human *CCR2B* knock-in (shown as h*CCR2B* KI) mice. Human *CCR2B* knock-in mice were injected with tdTomato-labeled E0771 cancer cell line into the tail vein, and two days later, MK0812 was administered orally (15 mg/kg, twice daily) for eight days. (B) Flow cytometry analysis of M-MDSCs in lungs ten days after tail vein injection of tdTomato-labeled E0771 cancer cell line. ***$p < 0.001$ (unpaired two-sided Student's t-test). ($N = 3$ for Control; $N = 4$ for MK0812). (C) Lung metastases were evaluated ten days after tail vein injection of tdTomato-labeled E0771 cancer cell line. Lungs were photographed under blue light irradiation (left). The percentage of tdTomato-positive cells of viable cells was analyzed by flow cytometry. (right). *$p < 0.05$ (unpaired two-sided Student's t-test). Scale bars: 5 mm. ($N = 3$ for Control; $N = 4$ for MK0812).

Oligonucleotides	**Figure**	
5’ -AUCAUCGUAGUCAUACGGUGGUUUUAGAGC UAUGCU-3’	1A	crRNA for CRISPR electroporation
5’-ATGCAAGTTCAGCTGCCTG-3’	1B, 1C, 3B and 3F	Forward primer for mouse CCR2 detection
5’-TGCATGGCCTGGTCTAAGTG-3’	1B and 1C	Reverse primer for mouse CCR2 detection
5’-CACCATCATCGTAGTCATACGGTG-3’	3A	Oligonucleotides of the mouse CCR2 sgRNA target
5’-AAACCACCGTATGACTACGATGAT-3’	3A	Oligonucleotides of the mouse CCR2 sgRNA target
5’-CACCGGGAGCAAGAGGTCTCGGTT-3’	3A	Oligonucleotides of the mouse CCR2 sgRNA target
5’-AAACAACCGAGACCTCTTGCTCCC-3’	3A	Oligonucleotides of the mouse CCR2 sgRNA target
5’-TCTCACTGCCCTATGCCTCT-3’	3B	Reverse primer for human CCR2B detection
5’-GAACTCGAGGAGCGGTGAAGAAGTCACCA-3’	3C	Forward primer for southern blot probe synthesis
5’-GGGAATTCCAGAAGCAAACACAGCCACC-3’	3C	Reverse primer for southern blot probe synthesis
5’-ATGAGGACGACCAGCATGTTG-3’	3F	Reverse primer for mouse human CCR2B detection
5’-CATCATCGTAGTCGTGTGGTG-3’		Genotyping of CCR2 knockout mice

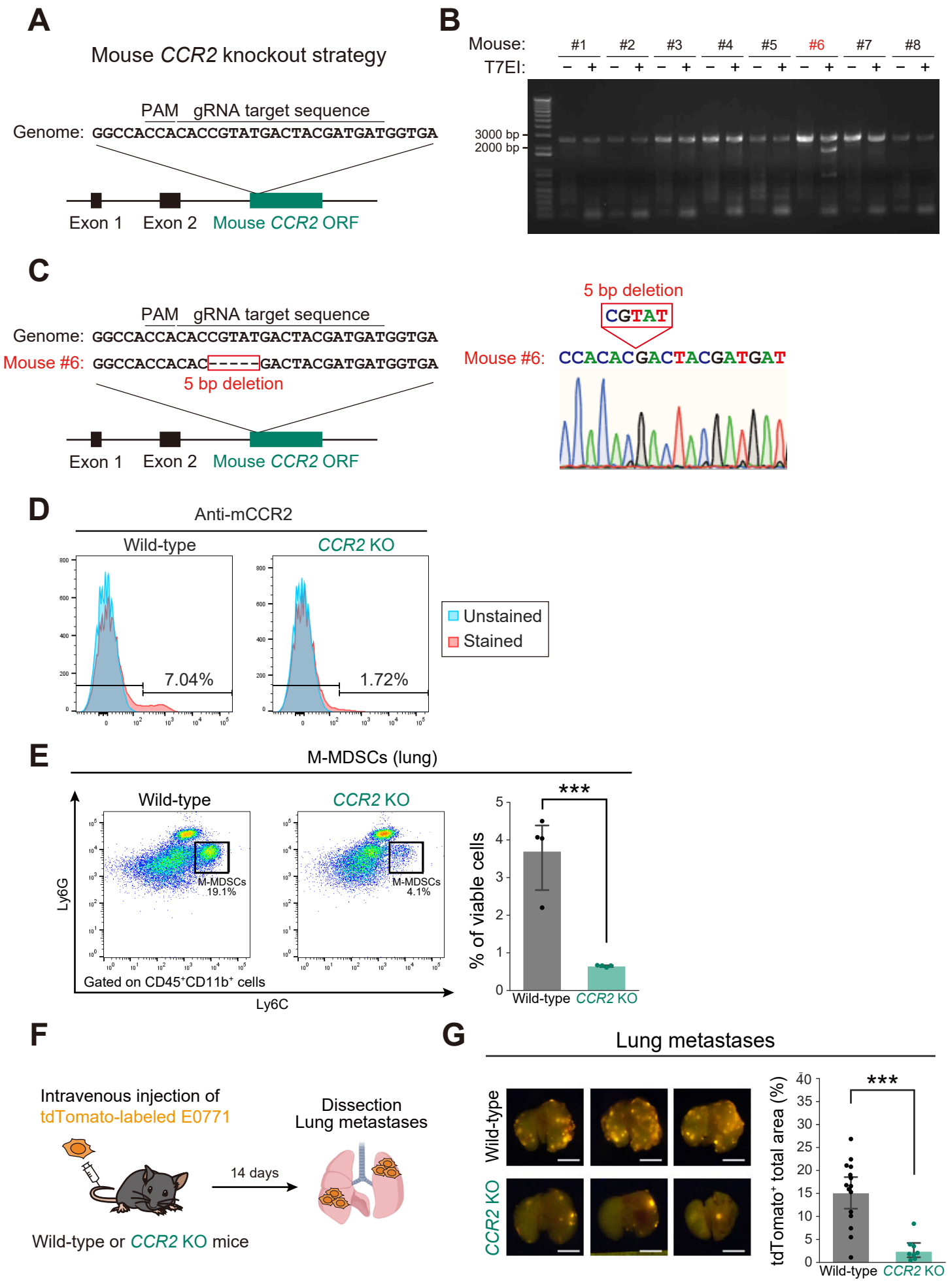
A
Mouse CCR2 knockout strategy
PAM
gRNA target sequence
Genome: GGCCACCACACCGTATGACTACGATGATGGTGA
Exon 1
Exon 2
Mouse CCR2 ORF
B
Mouse:
#1
#2
#3
#4
#5
#6
#7
#8
T7EI:
3000 bp
2000 bp
C
PAM
gRNA target sequence
Genome: GGCCACCACACCGTATGACTACGATGATGGTGA
Mouse #6: GGCCACCACAC-----GACTACGATGATGGTGA
5 bp deletion
Exon 1
Exon 2
Mouse CCR2 ORF
5 bp deletion
CGTAT
Mouse #6: CCACACGACTACGATGAT
D
Anti-mCCR2
Wild-type
CCR2 KO
7.04%
1.72%
Unstained
Stained
E
M-MDSCs (lung)
Wild-type
CCR2 KO
M-MDSCs
19.1%
M-MDSCs
4.1%
Ly6G
Gated on CD45+CD11b+ cells
Ly6C
***
% of viable cells
Wild-type
CCR2 KO
F
Intravenous injection of
tdTomato-labeled E0771
14 days
Dissection
Lung metastases
Wild-type or CCR2 KO mice
G
Lung metastases
Wild-type
CCR2 KO
***
tdTomato+ total area (%)
Wild-type
CCR2 KO

A

Ten existing human CCR2 inhibitors

- MK0812
- PF04634817
- INCB8761
- INCB3344
- Cenicriviroc
- JNJ2714149
- CCR2-RA-[R]
- CAS 445479-97-0
- RS504393
- RS102895

Comparison of human CCR2 inhibitory activity

- Fura 2-AM (Ca^{2+} selective fluorescent indicator)
- THP-1 (hCCR2-expressing human monocytic leukemia cell line)
- Recombinant human CCL2
- Each human CCR2 inhibitor

B

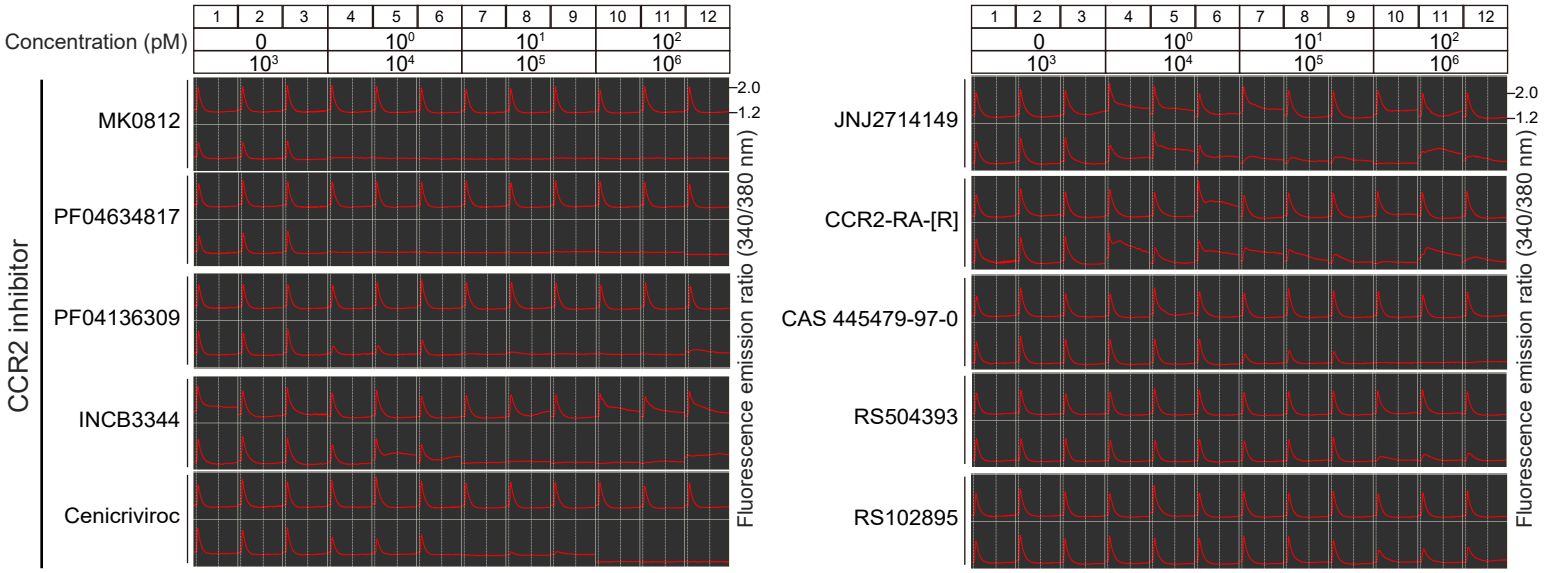

C

Ranking	CCR2 inhibitor	Mean IC_{50} (nM)
1	MK0812	1.73
2	PF04634817	2.52
3	PF04136309	6.99
4	INCB3344	13.67
5	Cenicriviroc	26.84
6	JNJ2714149	28.35
7	CCR2-RA-[R]	51.63
8	CAS 445479-97-0	66.19
9	RS504393	486.06

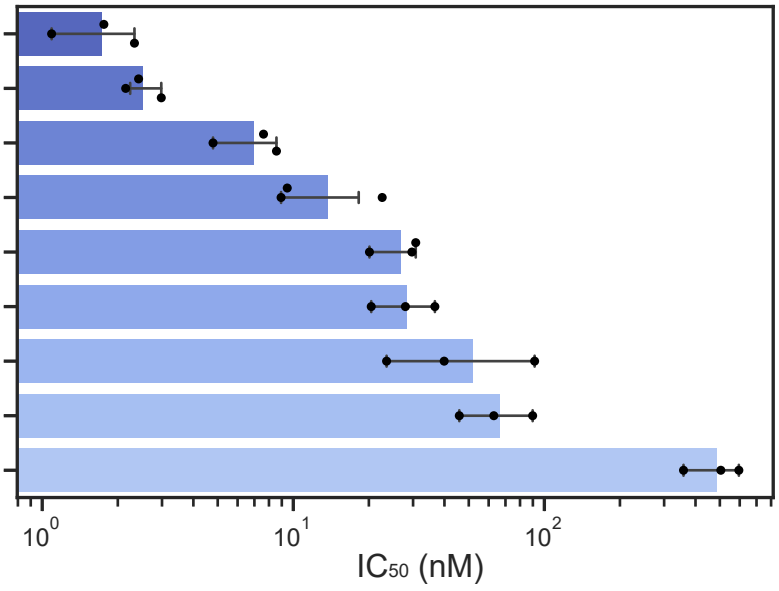

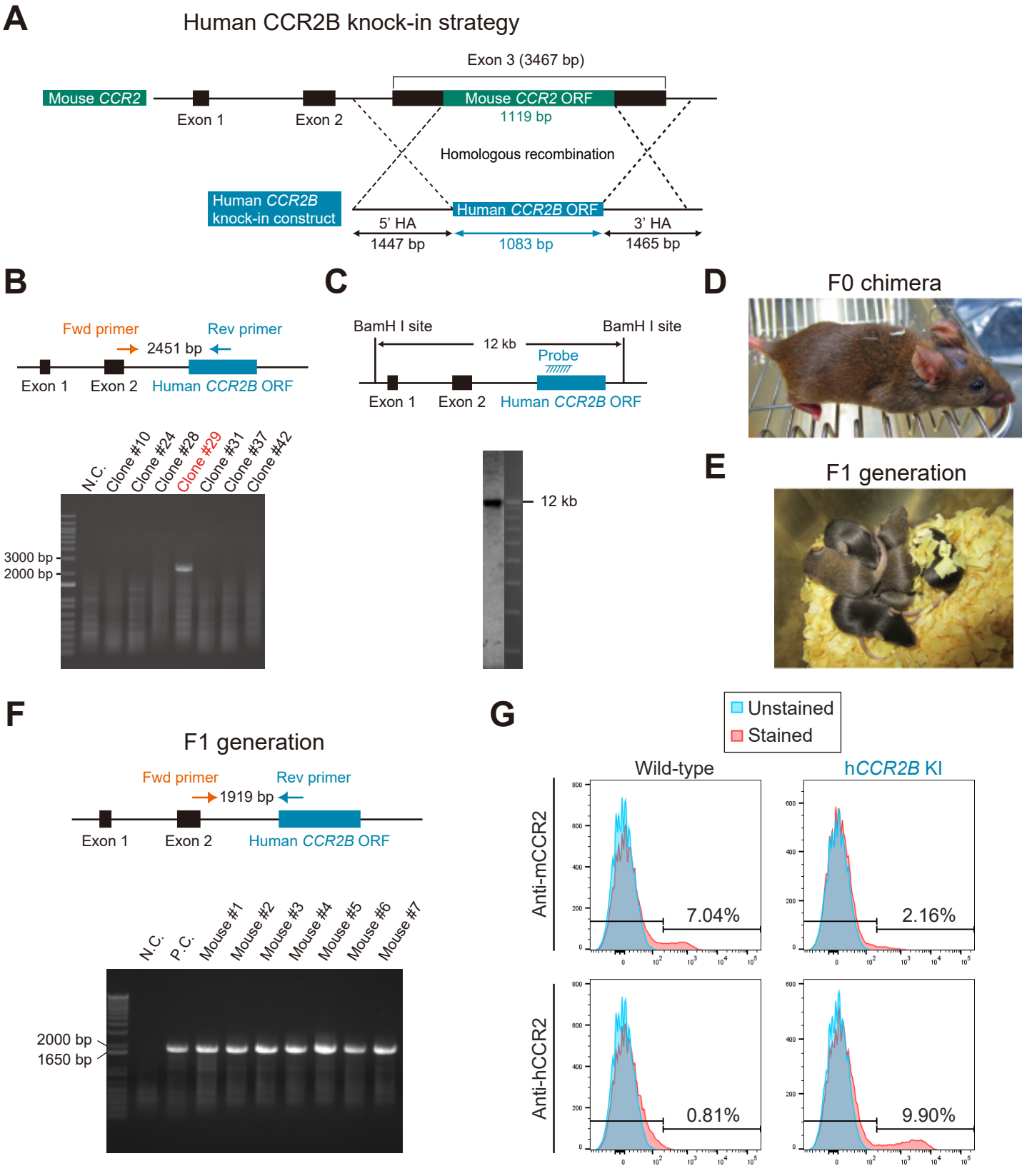
A
Human CCR2B knock-in strategy
Exon 3 (3467 bp)
Mouse CCR2
Exon 1
Exon 2
Mouse CCR2 ORF
1119 bp
Homologous recombination
Human CCR2B knock-in construct
Human CCR2B ORF
5' HA
1447 bp
1083 bp
3' HA
1465 bp
B
Fwd primer
Rev primer
2451 bp
Exon 1
Exon 2
Human CCR2B ORF
N.C.
Clone #10
Clone #24
Clone #28
Clone #29
Clone #31
Clone #37
Clone #42
3000 bp
2000 bp
C
BamH I site
12 kb
BamH I site
Probe
Exon 1
Exon 2
Human CCR2B ORF
12 kb
D
F0 chimera
E
F1 generation
F
F1 generation
Fwd primer
Rev primer
1919 bp
Exon 1
Exon 2
Human CCR2B ORF
N.C.
P.C.
Mouse #1
Mouse #2
Mouse #3
Mouse #4
Mouse #5
Mouse #6
Mouse #7
2000 bp
1650 bp
G
Unstained
Stained
Wild-type
hCCR2B KI
Anti-mCCR2
7.04%
2.16%
Anti-hCCR2
0.81%
9.90%

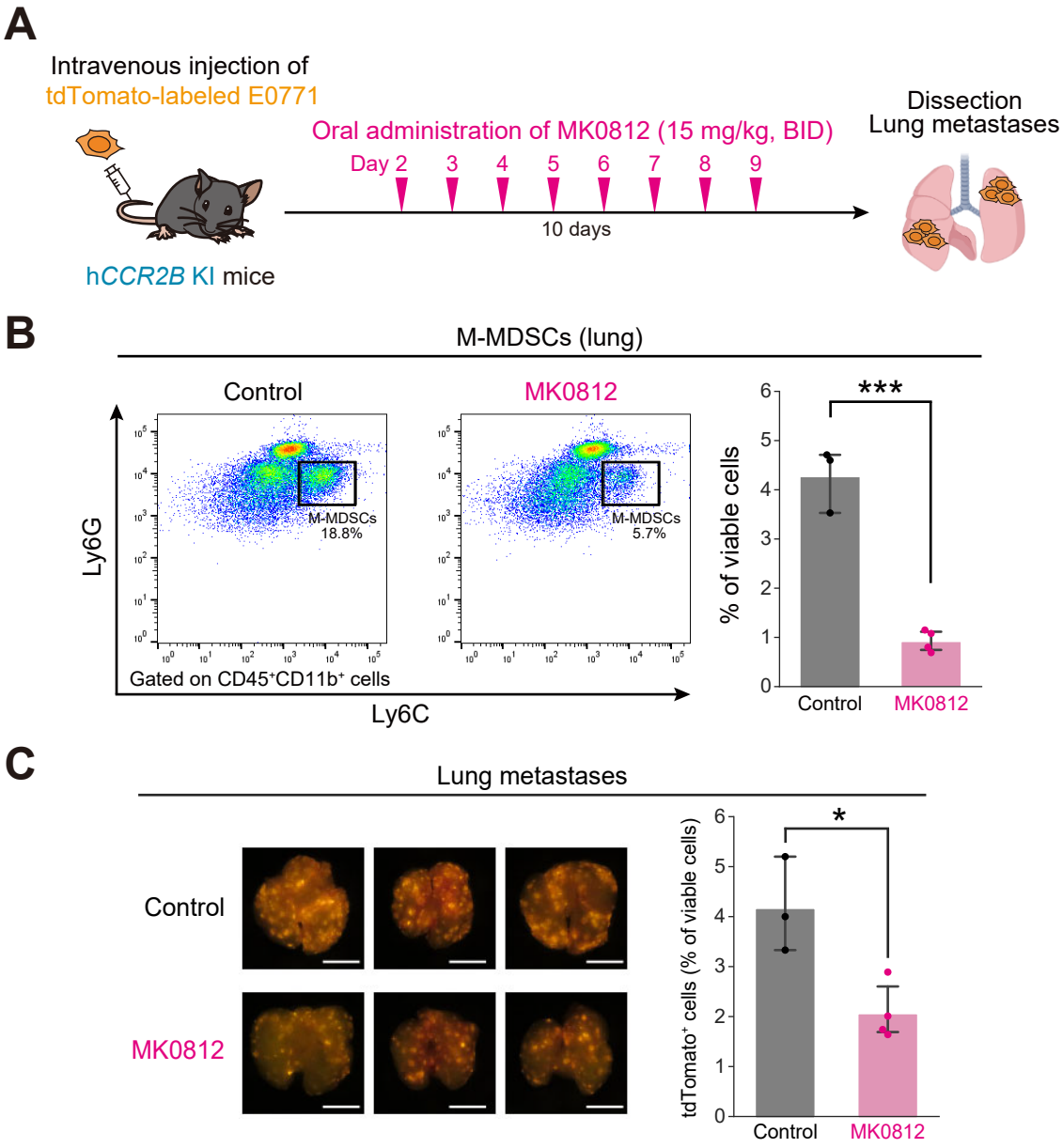
A
Intravenous injection of
tdTomato-labeled E0771
hCCR2B KI mice
Oral administration of MK0812 (15 mg/kg, BID)
Day 2 3 4 5 6 7 8 9
10 days
Dissection
Lung metastases
B
M-MDSCs (lung)
Control
MK0812
Ly6G
Ly6C
M-MDSCs
18.8%
M-MDSCs
5.7%
Gated on CD45+CD11b+ cells
% of viable cells
***
Control
MK0812
C
Lung metastases
Control
MK0812
tdTomato+ cells (% of viable cells)
*
Control
MK0812

Comparison of
10 human CCR2 inhibitors in vitro

IC_{50} ranking table

CCR2 inhibitor	IC_{50} (nM)	Ranking
MK0812	**1.73**	**1**
PF04634817	2.52	2
PF04136309	6.99	3
INCB3344	13.67	4
Cenicriviroc	26.84	5
JNJ2714149	28.35	6
CCR2-RA-[R]	51.63	7
CAS 445479-97-0	66.19	8
RS504393	486.06	9

Generation of
human CCR2 knock-in mice

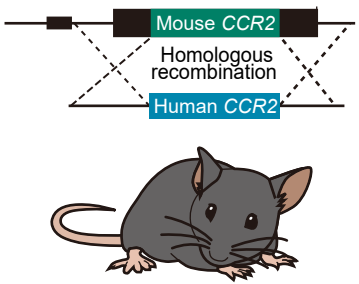

Human *CCR2* knock-in mice

Validation of **MK0812** in a cancer metastasis model
using **human CCR2 knock-in mice**